

ModQuad-DoF: A Novel Yaw Actuation for Modular Quadrotors

Bruno Gabrich¹, Guanrui Li¹, and Mark Yim¹.

Abstract—In this work we introduce ModQuad-DoF, a modular flying robotic structure with enhanced capabilities for yaw actuation. We propose a new module design that allows a one degree of freedom relative motion between the flying robot and the cage, with a docking mechanism allowing rigid connections between cages. A novel method of yaw actuation that increases the structure control authority is also presented. Our new method for the structure yaw control relies on the independent roll angles of each one of the modules, instead of the traditional drag moments from the propellers. In this paper, we propose a controller that allows the ModQuad-DoF to control its position and attitude. In our experiments, we tested a different number of modules flying in cooperation and validated the novel yaw actuation method.

I. INTRODUCTION

In nature it is very common for insects to work together in collaboration to achieve formation of structures such as bridges, platforms and other configurations. There is no centralized command that determines each individual's motions, forces and connections, once each one of them determines its own behavior locally. Similar cooperation with quadrotors has been introduced in [1] and also explored in [2] and [3]. Oung et.al [4] introduced a group structure concept where single propellers join on the ground to form a structure that can fly. A flying modular platform called *ModQuad* was shown to assemble in midair and cooperatively fly as a larger structure [2] [5]. This work was extended in [6], in which a non-rigid structure, composed of modules, was able to grasp objects.

Scaling modular robots [7],[8],[9] is a very challenging problem that usually limits the benefits of modularity. The sum of the performance metrics (speed, torque, precision etc.) from each module usually does not scale at the same rate as the conglomerate physical properties. In particular, for *ModQuad*, saturation from individual motors would increase as the structures became larger leading to failure and instability. In [2] specific configurations were not capable to maintain stable flight due to the lack of control authority especially for yaw motions as more modules were connected to the current flying structure. In the control of the flying structures with quadrotor-like architectures, yaw has been shown to be an issue especially as more actuators are added



Fig. 1. Six modules flying in a line configuration.

[10],[6]. In [6], [11] and [12] the control authority issue was solved by tilting the propellers of each module fifteen degrees off axis. This tilt gave some coupling of thrust directly to yaw without losing too much vertical thrust. Tilting further starts to reduce the overall thrust capability and increases power consumption [13], so there is a limit to how much yaw authority can be gained. This solution of tilting propellers still limits yaw actuation, since only half of the total number of propellers produces moments around z -axis for one direction.

When conglomerate systems scale up in the number of modules, the moment of inertia of the conglomerate often grows faster than the increase in thrust capability for each module. For example, the increase in the moment of inertia for a fifth module added to four modules in a line can be approximated by the mass of the module times half the distance to the center squared. This quadratic increase give us the intuition that the required yaw actuation grows faster than the actuation authority.

In this work, we propose a new module design that enables an added degree of freedom roll motion between joined modules in a conglomerate. In situations that two or more flying robots are connected together, the added DOF can be used to gain increased yaw authority without impacting individual module performance. The modules can dynamically tilt themselves rather than just the previous solution of fixed propellers at fifteen degrees along the roll axis to utilize the full thrust to gain yaw authority.

The contributions of this paper are twofold. *i)* We present a new design, dynamical model and a novel modular flying robot with increased yaw actuation when joined with others. *ii)* We propose a new kind of controller and a decentralized method to control the attitude of the conglomerate.

¹ B. Gabrich, G. Li and M. Yim are with the GRASP Laboratory, University of Pennsylvania, Philadelphia, PA, USA: {brunot, yim}@seas.upenn.edu, lguanrui@alumni.upenn.edu.

The authors gratefully acknowledge the support of DARPA grant HR00111520020, ONR grants N00014-15-1-2115 and N00014-14-1-0510, ARL grant W911NF-08-2-0004, NSF grant IIS-1426840, NSF grant 1138847, and TerraSwarm, one of six centers of STARnet, a Semiconductors Research Corporation program sponsored by MARCO and DARPA.

II. DESIGN AND MECHANICAL SYSTEM

Previous work [2], [6], [5] presented modular designs that encapsulates the quadrotor by rigidly attaching a cage to the flying vehicle. This cage has magnets that allow cages to dock together. Here, we propose a new type of design in which the modular cage and flying vehicle does not necessarily share same orientation. Although our design is novel, it still preserves similar docking capabilities as in [2] and [5], allowing modules to dock with other modules through permanent magnets.

A. Flying Vehicle

The Crazyflie 2.0 is the chosen platform to enable thrust and attitude to the individual modules. The flying vehicle measures $92 \times 92 \times 29$ mm and weights 27 g while its battery lasts around 4 minutes for the novel design proposed.

In this work the cage performs as pendulum relative to the flying vehicle. The quadrotor is joined to the cage through a one DOF joint (Fig. 2). The cages are made of light-weight materials: ABS for the 3-D printed connectors and joints, and carbon fiber for the rods.

B. Docking mechanism

Although the flying vehicle does not necessarily share same orientation as the cage, the multiple connected cages do preserve same orientation relative to each other. With the purpose of allowing such behavior, we used Neodymium Iron Boron (NdFeB) magnets as passive actuators to enable rigid cage connections. Docking is only allowed at the back and front face of the modules, and each one of these faces contains four magnets. Those passive actuators have dimensions of $6.35 \times 6.35 \times 0.79$ mm with a bonding force of 1 kg.

C. System Motion

The new system design allows the cage to behave as a passive pendulum relative to the quadrotor. The choice to enable docking only on the back and front faces was a design decision to minimize the cage total weight. Docking enabled on all four faces would require more material at a further distance from the pendulum axis of rotation relative to the flying vehicle. This could introduce more inertia to the system and disturbance that the robot could not reject. Even though the model presents oscillations between cage and flying vehicle our dynamics (Section IV) and control (Section VI) handle this disturbance since the oscillation amplitude is small.

III. MODQUAD-DOF MODEL

The flying conglomerate is formulated through the definition of the three following components.

Definition 1 (Module). A module is composed of a cage and a flying robot. Each module can move by itself in a three dimensional environment and dock horizontally to other modules on the back and front faces only.

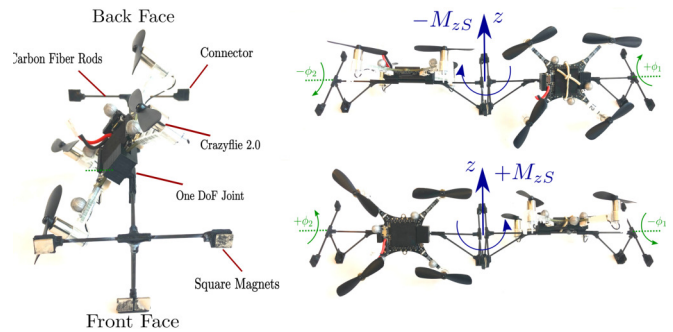


Fig. 2. The ModQuad-DoF module is composed of square magnets, carbon fiber rods, mocap markers, 3-D printed connectors and a one degree of freedom joint.

Definition 2 (Structure). A structure is composed of n modules rigidly attached to each other in a line configuration.

Definition 3 (Line Configuration). A line configuration is a structure in which the addition of modules increases its dimension along a single axis only.

A structure is formed by n modules, indexed by $i = 1, \dots, n$. In Fig. 3 the structure frame is represented by \mathcal{S} and the modules frames by \mathcal{M}_i . $\mathbf{r}_S, \dot{\mathbf{r}}_S, \ddot{\mathbf{r}}_S \in \mathbb{R}^3$ represents the structure position, linear velocity and linear acceleration in the world frame \mathcal{W} . The structure attitude is represented by $\Theta_S = [\phi_S, \theta_S, \psi_S]^\top$ while Ω_S and $\dot{\Omega}_S$ the angular velocity and acceleration respectively. Analogous to the structure, $\mathbf{r}_i = [r_{x_i}, r_{y_i}, r_{z_i}]^\top$ represents the position of module i in \mathcal{S} , while $\Theta_i = [\phi_i, \theta_i, \psi_i]^\top$, $\Omega_i = [\dot{\phi}_i, \dot{\theta}_i, \dot{\psi}_i]^\top$ and $\dot{\Omega}_i = [\ddot{\phi}_i, \ddot{\theta}_i, \ddot{\psi}_i]^\top$ are attitude, angular velocity and angular acceleration of each module. The structure inertia tensor is defined by \mathbf{I}_S and \mathbf{I} is the tensor for each individual module.

Each module i is equipped with four rotors, indexed by $j = 1, \dots, 4$, that produce angular speeds ω_{ij} to generate forces in \mathcal{S}

$$f_{ij} = K_f \cos(\phi_i) \omega_{ij}^2, \text{ for } n > 1,$$

and moments in \mathcal{S}

$$M_{ij} = \pm K_f \sin(|\phi_i|) |x_{ij}| \omega_{ij}^2, \text{ for } n > 1,$$

where n is the total number of modules i in the structure, K_f is a motor constants that can be obtained experimentally, x_{ij} represents the distance in \mathcal{S} from motor j of module i to the center of mass of the conglomerate, and ϕ_i is the independent roll attitude angle for module i .

IV. MODQUAD-DOF DYNAMICS

Based on the actuators forces, we can write the translational dynamics for the structure center of mass as

$$nm\ddot{\mathbf{r}}_S = \begin{bmatrix} 0 \\ 0 \\ -nmg \end{bmatrix} + \mathbf{R}_S^{\mathcal{W}} \sum_{ij} \mathbf{R}_{\mathcal{M}_i}^{\mathcal{S}} \begin{bmatrix} 0 \\ 0 \\ f_{ij} \end{bmatrix},$$

where $\mathbf{R}_S^{\mathcal{W}}$ is a rotation matrix from the world coordinate frame \mathcal{W} to the structure frame \mathcal{S} , and $\mathbf{R}_{\mathcal{M}_i}^{\mathcal{S}}$ is the rotation matrix from \mathcal{S} to each individual module frame \mathcal{M}_i . This

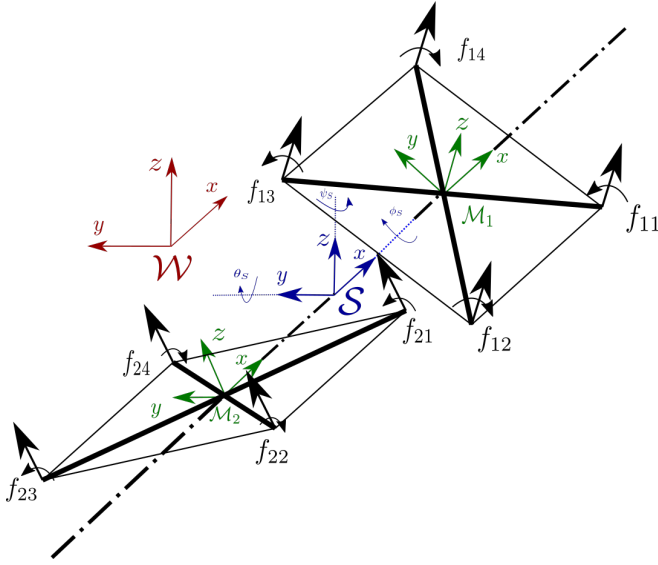


Fig. 3. A structure diagram composed of two modules. The modules do not share the same orientation and are rotated around the structure x -axis. The black arrows represents the force and direction produced by the propellers while the cross within the squares represents the quadrotors.

rotation is modelled by the Z-X-Y Euler angles convention, where m is the mass of each individual module and g is the acceleration of gravity.

The rotational dynamics can be represented as follows

$$\mathbf{I}_S \dot{\boldsymbol{\Omega}}_S = \mathbf{M}_S = \sum_i \begin{bmatrix} 0 & 0 & 0 \\ 0 & 1 & 0 \\ -\chi(r_{x_i}) & 0 & 0 \end{bmatrix} \mathbf{R}_{\mathcal{M}_i}^S \mathbf{M}_i,$$

$\chi(x) = x/|x|$, $\mathbf{M}_S = [M_{xS}, M_{yS}, M_{zS}]^\top$, and $\mathbf{M}_i = [M_{xi}, M_{yi}, 0]^\top$ representing local moment contributions. The inertia tensor for the structure \mathbf{I}_S can be computed by the sum of the inertia contribution from each individual module i as $\mathbf{I}_S = \sum_{i=1}^n \mathbf{I}_i$. This contribution can be obtained through the parallel axis theorem and by reorienting the inertia of the i th module according to frame \mathcal{S} . Thus, for a line configuration we can write it as

$$\mathbf{I}_i = \mathbf{R}_{\mathcal{M}_i}^S \mathbf{I}_{\mathcal{S}}^{\mathcal{M}_i} + m \begin{bmatrix} 0 & 0 & 0 \\ 0 & r_{x_i}^2 & 0 \\ 0 & 0 & r_{x_i}^2 \end{bmatrix},$$

where $\mathbf{I} = \text{Diag}([I_x, I_y, I_z])$, r_{x_i} is the first element of the position vector \mathbf{r}_i and $\mathbf{R}_{\mathcal{M}_i}^S$ can be defined as \mathbf{R}_{x, ϕ_i} .

Lastly, we describe how individual motor forces affects the structure moments.

$$\mathbf{M}_S = \sum_{ij} \left([x_{ij} \ 0 \ 0]^\top \times \mathbf{R}_{\mathcal{M}_i}^S [0 \ 0 \ f_{ij}]^\top \right),$$

where x_{ij} represents motors x -coordinate position in the structure frame. Differently from [2] and [5] the structure forces and moments are also a function of the roll angle of the i th module.

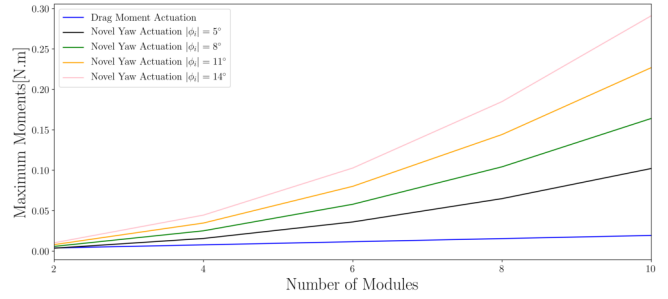


Fig. 4. Yaw actuation scaling comparison. The maximum moment produced by the drag moment actuation is compared to the new yaw actuation method for $|\phi_i| = 5^\circ$, $|\phi_i| = 8^\circ$, $|\phi_i| = 11^\circ$, and $|\phi_i| = 14^\circ$. The studied case consider a structure in a line configuration for a hovering condition.

V. MOMENTS IN Z SCALING ANALYSIS

In this section the structure yaw actuation scalability is analysed. A comparison with different number of modules is performed for drag moments and the new method of yaw actuation.

An inherit characteristic of quadrotors is to have their yaw controlled by the drag moments from each propeller. For *ModQuad* as more modules are docked together, a decreased controllability in yaw is noticed as the structure becomes larger. In a line configuration the structure's inertia grows quadratically with the distance of each module to the structure center of mass. On the other hand the drag moments produced scales linearly with the number of modules. Under hovering conditions and for an even number of modules in a line, it can be defined as follows

$${}^D M_{zS} = 8nK_m \bar{w} (\delta w)_{max}, \text{ s.t. } n = 2k \text{ for } k \in \mathbb{Z},$$

where K_m is a motor constant that can be obtained experimentally, \bar{w} is the angular speed of each propeller in hovering condition [14] and, δw_{max} is the maximum angular speed deviation from the hovering condition in order to generate maximum moments around the z -axis. The rate difference in which drag moments and inertia increases, brings limitations to the platform in the sense that some specific configurations could not be achieved given the control authority constrain. Therefore, a different method of actuation that is capable to overcome such limitations is desired.

The new yaw actuation method relies on the fact that each quadrotor is capable to generate an individual ϕ_i enabled by the new cage design described in Section II. By working in coordinated manner, each quadrotor can then generate structure moments from moment arms provided by the propellers given its ϕ_i and its distance from the structure's center of mass. The computation of such moments under hovering conditions for a line configuration can be achieved as follows

$${}^N M_{zS} = K_f \bar{w}^2 \sum_i^n \tan |\phi_i| \sum_j^4 |x_{ij}|.$$

For simplicity and specifically for this comparison analysis, a solution in which the magnitude of all ϕ_i are equal

is adopted. Fig. 4 shows a comparison between the two methods of actuation as the number of modules in a line configuration becomes larger. Both drag moments and new actuation method are illustrated, given that the latter is performed for three specific angles. We observe that the actuation for the new method grows at a faster rate as the number of modules increases and, depending on the applied ϕ_i , the structure yaw authority could be considerably improved.

VI. MODQUAD-DOF CONTROL

The structure yaw control method relies on the independent roll of each robot, that if applied in coordinated manner generates enough moments for the structure. Therefore, in this section we describe how our new method of actuation is achieved and how the control is implemented for n modules forming a line configuration.

The control consists of a centralized trajectory control, a structure force distribution and a decentralized attitude controller.

A. Centralized Trajectory Control

Initially, a centralized trajectory control for the structure is applied. The position control is achieved by the computation of the desired linear accelerations given linear position, velocity and acceleration generated by the trajectory. The computation of the desired linear accelerations in \mathcal{W} is achieved as follows

$$\ddot{\mathbf{r}}_S^* = \mathbf{K}_{pS}(\mathbf{r}_{S,T} - \mathbf{r}_S) + \mathbf{K}_{dS}(\dot{\mathbf{r}}_{S,T} - \dot{\mathbf{r}}_S) + \ddot{\mathbf{r}}_{S,T},$$

where $\mathbf{K}_{pS} = \text{Diag}([K_{pxS}, K_{pyS}, K_{pzS}])$ and $\mathbf{K}_{dS} = \text{Diag}([K_{dxS}, K_{dyS}, K_{dzS}])$ are the diagonal matrices of proportional and derivative gains respectively. Further, $\mathbf{r}_{S,T}$, $\dot{\mathbf{r}}_{S,T}$, $\ddot{\mathbf{r}}_{S,T}$ are position, velocity and acceleration in the desired trajectory. Given n modules, the desired force vector for the structure in \mathcal{S} is computed as follows

$$\mathbf{F}_S^{*\mathcal{S}} = nm\mathbf{R}_{\mathcal{W}}^S(\mathbf{g} + \ddot{\mathbf{r}}_S^*), \quad (1)$$

where $\mathbf{F}_S^{*\mathcal{S}} = [F_{xS}^{*\mathcal{S}}, F_{yS}^{*\mathcal{S}}, F_{zS}^{*\mathcal{S}}]^\top$. It is important to notice that at this stage, the centralized control strategy assumes that all modules share same orientation as the structure.

B. Structure Force Distribution for Yaw Control

With the purpose to apply our new method of actuation, the component $\mathbf{F}_S^{*\mathcal{S}}$ is distributed to each module, given its location in frame \mathcal{S} . This distribution can be achieved as follows

$$\begin{bmatrix} \mathbf{F}_S^{*\mathcal{S}} \\ \mathbf{M}_{zS}^{*\mathcal{S}} \end{bmatrix} = \mathbf{S}\mathbf{F}^{*\mathcal{S}}, \quad (2)$$

where $\mathbf{F}^{*\mathcal{S}} = [F_{x1}^{*\mathcal{S}}, F_{y1}^{*\mathcal{S}}, F_{z1}^{*\mathcal{S}}, \dots, F_{xn}^{*\mathcal{S}}, F_{yn}^{*\mathcal{S}}, F_{zn}^{*\mathcal{S}}]^\top$, $\mathbf{S} \in \mathbb{R}^{4 \times 3n}$ is a matrix that converts modules desired forces to structure desired force and desired moment around the z -axis. It can be defined as

$$\mathbf{S} = \begin{bmatrix} \mathcal{I} & \dots & \mathcal{I} \\ \mathbf{r}_{x1} & \dots & \mathbf{r}_{xn} \end{bmatrix},$$

where $\mathcal{I} \in \mathbb{R}^{3 \times 3}$ is an identity matrix and $\mathbf{r}_{x_i} = [0, r_{x_i}, 0]$. From (1) only desired force is obtained. Therefore a proportional-derivative controller is applied to compute the structure desired moment in z as follows

$$M_{zS}^{*\mathcal{S}} = k_{p\psi}(\psi_{S,T} - \psi_S) + k_{d\dot{\psi}}(\dot{\psi}_{S,T} - \dot{\psi}_S), \quad (3)$$

where $\psi_{S,T}$, $\dot{\psi}_{S,T}$ are structure yaw angle and yaw rate in the desired trajectory, $k_{p\psi}$ and $k_{d\dot{\psi}}$ are proportional and derivative gains. In reality we need to obtain $\mathbf{F}^{*\mathcal{S}}$, therefore the transformation presented (2) is inverted. Since \mathbf{S} is not a square matrix, a pseudo-inverse solution is chosen. This solution will result in minimizing the norm of $\mathbf{F}^{*\mathcal{S}}$. Thus, it can be defined as

$$\mathbf{F}^{*\mathcal{S}} = \mathbf{S}^\top (\mathbf{S}\mathbf{S}^\top)^{-1} \begin{bmatrix} \mathbf{F}_S^{*\mathcal{S}} \\ M_{zS}^{*\mathcal{S}} \end{bmatrix}, \quad (4)$$

C. Thrust and Decentralized Attitude Computation

Given the computed desired force vectors in (4), a transformation to the world frame \mathcal{W} is accomplished as follows

$$\mathbf{F}_i^* = \mathbf{R}_S^{\mathcal{W}} [F_{ix}^{*\mathcal{S}}, F_{iy}^{*\mathcal{S}}, F_{iz}^{*\mathcal{S}}]^\top,$$

hence, the desired thrust for each individual module can be obtained as

$$F_i = \mathbf{F}_i^* \cdot \mathbf{R}_{\mathcal{M}_i}^{\mathcal{W}} \mathbf{e}_3, \quad (5)$$

where $\mathbf{e}_3 = [0, 0, 1]^\top$. The desired orientation for each module i is computed through a rotation matrix defined as follows

$$\mathbf{R}_{\mathcal{M}_i}^* = [\mathbf{b}_{i1}^* \quad \mathbf{b}_{i2}^* \quad \mathbf{b}_{i3}^*],$$

in which, each \mathbf{b}_{i3}^* has the same direction as \mathbf{F}_i^* and can be computed as follows

$$\mathbf{b}_{i3}^* = \mathbf{F}_i^* / \|\mathbf{F}_i^*\|.$$

In traditional geometric control [5], [15], [16] \mathbf{b}^{yaw} is a function of the desired yaw. Although, in this work $\mathbf{b}^{yaw} = [\cos \psi_S, \sin \psi_S, 0]^\top$. In other words, \mathbf{b}^{yaw} is a function of the current structure yaw. Further, we define \mathbf{b}_{i1}^* and \mathbf{b}_{i2}^* which are functions of \mathbf{b}_{i3}^* and \mathbf{b}^{yaw} as

$$\mathbf{b}_{i2}^* = \frac{\mathbf{b}_{i3}^* \times \mathbf{b}^{yaw}}{\|\mathbf{b}_{i3}^* \times \mathbf{b}^{yaw}\|}, \mathbf{b}_{i1}^* = \mathbf{b}_{i2}^* \times \mathbf{b}_{i3}^*,$$

thus, the desired angular accelerations for each module i can be obtained as follows

$$\ddot{\phi}_i = K_{p,\phi}(\phi_i^* - \phi_i) + K_{d,\dot{\phi}}(\dot{\phi}_i^* - \dot{\phi}_i), \quad (6)$$

$$\ddot{\theta}_i = K_{p,\theta}(\theta_i^* - \theta_i) + K_{d,\dot{\theta}}(\dot{\theta}_i^* - \dot{\theta}_i), \quad (7)$$

$$\ddot{\psi}_i = 0, \quad (8)$$

where $\phi_i^* = \text{atan2}(b_{2iz}^*, b_{3iz}^*)$ and $\theta_i^* = \sin^{-1}(b_{1iz}^*)$. It is worth noticing that ψ_i is always set to be zero. The yaw authority for the structure is commanded by an extra amplitude computed for ϕ_i^* originated in (4). Therefore, (6)-(8) can be written in a more compact form as follows

$$\dot{\Omega}_i = \mathbf{K}_{p,\Theta}(\Theta_i^* - \Theta_i) + \mathbf{K}_{d,\Omega}(\Omega_i^* - \Omega_i), \quad (9)$$

$\mathbf{K}_{p,\Theta} = \text{Diag}([K_{p,\phi}, K_{p,\theta}, K_{p,\psi}])$ and $\mathbf{K}_{d,\Omega} = \text{Diag}([K_{d,\phi}, K_{d,\theta}, K_{d,\psi}])$. The desired angular velocity

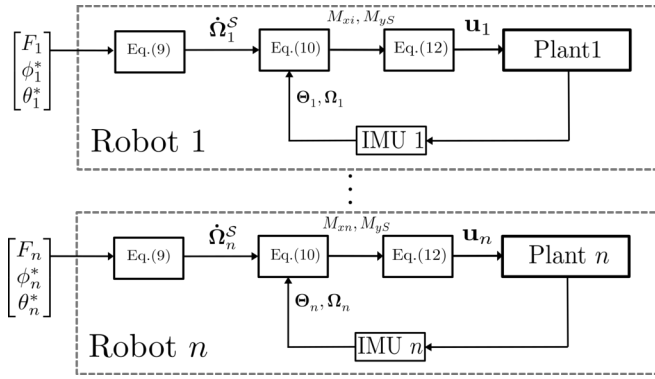


Fig. 5. ModQuad-DoF decentralized attitude controller diagram.

Ω_i^* is set to zero or defined by a trajectory. With $\dot{\Omega}_i$ obtained, the moments for each individual module can be computed as follows

$$[M_{xi} \ M_{yS} \ 0]^T = \mathcal{I}_0 \mathbf{I}_S \dot{\Omega}_i, \quad (10)$$

where $\mathcal{I}_0 = \text{Diag}([1, 1, 0])$. In order to distribute the forces to the rotors a similar method shown in [2], [5] is applied. This approach minimizes the maximum force required to achieve a desired moment in y . The equal force distribution around y can be written as follows,

$$f_{ij} = \frac{F_i}{4} + \frac{\chi(y_{ij})}{\sum_j |y_{ij}|} M_{xi} + \frac{\chi(x_{ij})}{\sum_{ij} |x_{ij}|} M_{yS}, \quad (11)$$

where $\chi(x) \equiv x/|x|$. The rotor forces $\mathbf{u}_i = [f_{i1}, f_{i2}, f_{i3}, f_{i4}]^T$, can be rewritten as follows

$$\mathbf{u}_i = \begin{bmatrix} \frac{1}{4} & c_{xi1} & c_{yi1} \\ \frac{1}{4} & c_{xi2} & c_{yi2} \\ \frac{1}{4} & c_{xi3} & c_{yi3} \\ \frac{1}{4} & c_{xi4} & c_{yi4} \end{bmatrix} \begin{bmatrix} F_i \\ M_{xi} \\ M_{yS} \end{bmatrix}, \quad (12)$$

where

$$c_{xij} = \frac{\chi(x_{ij})}{\sum_j |x_{ij}|}, c_{yij} = \frac{\chi(y_{ij})}{\sum_{ij} |y_{ij}|}.$$

Due to (8), the local moments around individuals z -axes is equal to zero.

In our controller approach we highlight that the structure desired force \mathbf{F}_S^* and desired moment M_{zS}^* are distributed to the n modules. Fig. (5) summarizes the decentralized attitude controller. Divergently from [2] and [5], the robots receive only thrust, roll and pitch, in which the magnitude of the second is not necessarily equal for all of them.

VII. EXPERIMENTS

In this section we aim to validate dynamic properties of ModQuad-DoF and the proposed controller. More specifically we are interested in showing the yaw behavior of the structure and the individuals roll angle and roll rate.

We use a Crazyflie-ROS node [17] with odometry obtained through a motion capture system (VICON) operated at 100 Hz. The high level commands are computed via ROS and sent at a rate of 50 Hz. Thrust and attitude commands are sent to each one of the robots via 2.4 GHz radio. Each

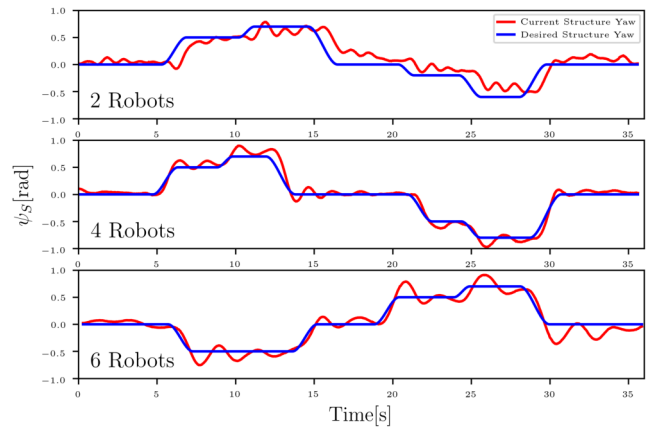


Fig. 6. Yaw performance for a structure composed of 2, 4, and 6 robots in a line configuration.

robot has a local IMU and attitude controller. Similarly to [2], [6], the crazyflie firmware was modified under its power distribution module in order to implement Eqs.(12), allowing the structure to cooperatively fly.

A. Structure Yaw Control

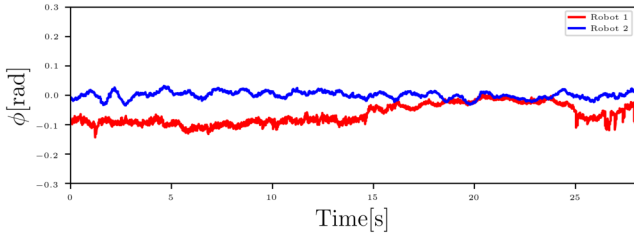
The structure yaw control experiment used the method presented in Section VI. Given that, appropriate thrust and attitude commands were sent to each one of the modules. The structure was intended to keep hovering in place while different desired yaw commands were set. Experiments were conducted for 2, 4 and 6 robots in a line configuration. For each one of those cases, a different tuning of (3) was required.

Fig. 6 shows the structure yaw behavior for three different numbers of modules. It is important to note that no drag moments from the propellers were used to control the conglomerate, once yaw actuation was provided by our proposed method. Another important fact to notice is that the yaw controllability for six modules in a line configuration was achieved. In [2] the yaw was uncontrollable whenever more than 4 robots were docked together in a line or whenever a considerable disturbance around the z -axis occurred.

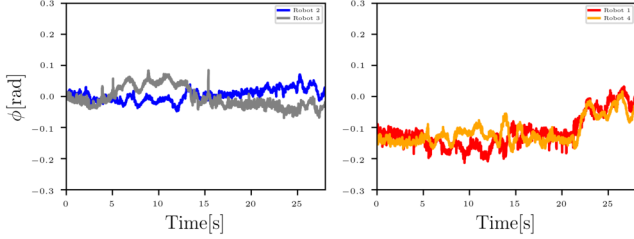
For the experiment with two robots, the structure received seven different commands for ψ_S^* , and for all of them the flying structure was able to achieve the commanded desired yaw. In the case of four robots, seven different ψ_S^* were sent, and similarly to the two robot case the flying structure approached to the desired state. In the six robot experiment six desired yaw angles were set. The structure followed the desired yaw trajectory, although more oscillations were noticed. Oscillations happened due to the controller tuning in (3). In fact, this type of response is an indication of the larger yaw control authority provided by our method.

B. Flying Robots Roll Angle

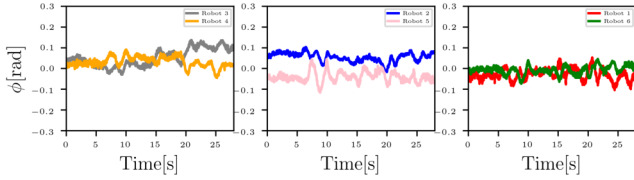
Fig. 7 shows the actual roll angles for the experiments of a structure composed of two, four and six robots. Small control gains were used to execute the structure yaw control



(a) Roll Angles for Robot 1 and 2.



(b) Roll Angles for Robot 1, 2, 3 and 4.



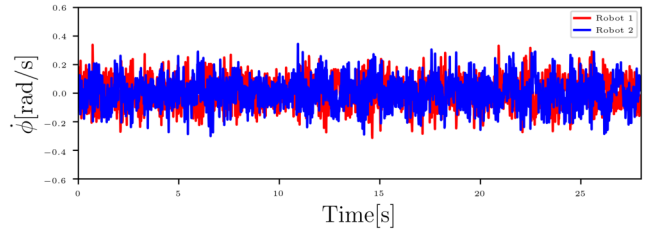
(c) Roll Angles for Robot 1, 2, 3, 4, 5 and 6.

Fig. 7. This plot represents the performance of roll angles for a structure composed of 2, 4 and 6 robots for different structure's yaw orientation.

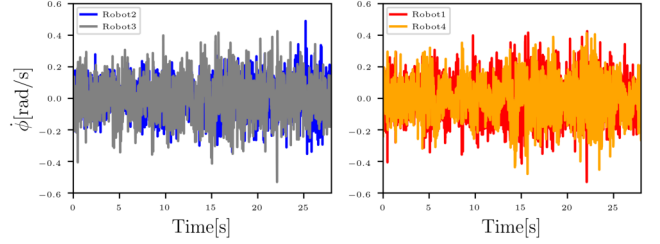
experiment, which caused the roll angles of each robot to be very small. Based on the analysis made on Section V, this was an expected behavior, given that even roll angles smaller than 5° could produce bigger moments compared to the drag moment actuation.

C. Flying Robots Roll Rate

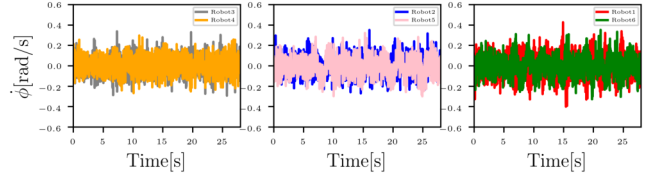
The solution proposed by applying matrix \mathbf{S} described in Section VI-B, minimizes the norm of $\mathbf{F}^* \mathbf{S}$. This minimization results in a linear distribution for F_{iy}^* , as well as equal solutions of F_{ix}^* and F_{iz}^* for all robots. Meaning that, individuals closer to the center of mass of the structure obtain smaller rolling angle magnitudes compared to the ones further. Fig. 8(b) shows that this type of solution has a direct correlation to the roll rate amplitude. For the structure composed of 4 robots, robot 1 and 4 are symmetrically located at the end of the structure, while robot 2 and 3 are closer to the structure's center of mass. Because robot 1 and 4 are further from the axis of rotation, they presented higher amplitudes for its roll rates, varying between $[-0.53 \text{ rad/s}, 0.43 \text{ rad/s}]$, while roll rates for robots 2 and 3 oscillated between $[-0.36 \text{ rad/s}, 0.48 \text{ rad/s}]$. Similarly, Fig. 8(c) presents the behavior in which 6 robots cooperatively fly in line configuration. Robots 1 and 6 are located at both ends of the structure, robot 2 is next to robot 1, robot 5 next to 6, and robots 3 and 4 are the closest to the structure's center of mass. Because of that, robots 3 and 4 presented



(a) Roll Rates for Robot 1 and 2.



(b) Roll Rates for Robot 1, 2, 3 and 4.



(c) Roll Rates for Robot 1, 2, 3, 4, 5 and 6.

Fig. 8. This plot represents the performance of roll rates for a structure composed of 2, 4 and 6 robots for different structure's yaw orientation.

roll rates of $[-0.29 \text{ rad/s}, 0.33 \text{ rad/s}]$, while robots 2 and 5 presented roll rates of $[-0.39 \text{ rad/s}, 0.35 \text{ rad/s}]$ and robots 1 and 6 presented roll rates of $[-0.40 \text{ rad/s}, 0.42 \text{ rad/s}]$.

VIII. CONCLUSION AND FUTURE WORK

In this paper, we introduce ModQuad-DoF, a flying modular robotic structure whose yaw actuation scales with increased numbers of modules. ModQuad-DoF has a one DOF jointed cage design and a novel control method for the flying structure. Our new yaw actuation method was validated conducting experiments for hovering conditions. We were able to perform two, four and, six modules cooperatively flying in a line with yaw controllability and reduced loss in thrust.

In future work we aim to explore the structure controllability with more robots in a line configuration, and exploring different solutions for the desired roll angles. Possibly, with more modules in the structure, only a few would be required to roll in order to maintain a desired structure yaw. Given that, we could explore the control allocation for each individual modules in specific structure configurations and dependent on the its behavior. Further, structures that are not constrained to a line will also be tested using a similar proposed controller.

REFERENCES

- [1] D. Mellinger, M. Shomin, N. Michael, and V. Kumar, "Cooperative grasping and transport using multiple quadrotors," *Springer Tracts in Advanced Robotics*, vol. 83 STAR, pp. 545–558, 2012.
- [2] D. Saldana, B. Gabrich, G. Li, M. Yim, and V. Kumar, "Modquad: The flying modular structure that self-assembles in midair," in *2018 IEEE International Conference on Robotics and Automation (ICRA)*. IEEE, 2018, pp. 691–698.
- [3] G. Loianno and V. Kumar, "Cooperative transportation using small quadrotors using monocular vision and inertial sensing," *IEEE Robotics and Automation Letters*, vol. 3, no. 2, pp. 680–687, 2017.
- [4] R. Oung and R. D'Andrea, "The distributed flight array," *Mechatronics*, vol. 21, no. 6, pp. 908–917, 2011. [Online]. Available: <http://dx.doi.org/10.1016/j.mechatronics.2010.08.003>
- [5] G. Li, B. Gabrich, D. Saldana, J. Das, V. Kumar, and M. Yim, "Modquad-vi: A vision-based self-assembling modular quadrotor," in *2019 International Conference on Robotics and Automation (ICRA)*. IEEE, 2019, pp. 346–352.
- [6] B. Gabrich, D. Saldana, V. Kumar, and M. Yim, "A flying gripper based on cuboid modular robots," in *2018 IEEE International Conference on Robotics and Automation (ICRA)*. IEEE, 2018, pp. 7024–7030.
- [7] K. Stoy, D. Brandt, and D. J. Christensen, *Self-reconfigurable robots: an introduction*. Mit Press, 2010.
- [8] M. Yim, D. G. Duff, and K. D. Roufas, "Polybot: a modular reconfigurable robot," in *ICRA*, 2000, pp. 514–520.
- [9] P. J. White and M. Yim, "Scalable modular self-reconfigurable robots using external actuation," in *2007 IEEE/RSJ International Conference on Intelligent Robots and Systems*. IEEE, 2007, pp. 2773–2778.
- [10] M. Zhao, K. Kawasaki, X. Chen, S. Noda, K. Okada, and M. Inaba, "Whole-body aerial manipulation by transformable multirotor with two-dimensional multilinks," in *Robotics and Automation (ICRA), 2017 IEEE International Conference on*. IEEE, 2017, pp. 5175–5182.
- [11] T. Anzai, M. Zhao, S. Nozawa, F. Shi, K. Okada, and M. Inaba, "Aerial grasping based on shape adaptive transformation by halo: Horizontal plane transformable aerial robot with closed-loop multilinks structure," in *2018 IEEE International Conference on Robotics and Automation (ICRA)*. IEEE, 2018, pp. 6990–6996.
- [12] D. Falanga, E. Mueggler, M. Faessler, and D. Scaramuzza, "Aggressive quadrotor flight through narrow gaps with onboard sensing and computing using active vision," in *Proc. of the IEEE International Conference on Robotics and Automation (ICRA)*, 2017.
- [13] C. Holda, B. Ghalamchi, and M. W. Mueller, "Tilting multicopter rotors for increased power efficiency and yaw authority," in *2018 International Conference on Unmanned Aircraft Systems (ICUAS)*. IEEE, 2018, pp. 143–148.
- [14] C. Luis and J. L. Ny, "Design of a trajectory tracking controller for a nanoquadcopter," *arXiv preprint arXiv:1608.05786*, 2016.
- [15] T. Lee, M. Leok, and N. H. McClamroch, "Nonlinear robust tracking control of a quadrotor uav on se (3)," *Asian Journal of Control*, vol. 15, no. 2, pp. 391–408, 2013.
- [16] D. Mellinger and V. Kumar, "Minimum snap trajectory generation and control for quadrotors," *Proceedings - IEEE International Conference on Robotics and Automation*, pp. 2520–2525, 2011.
- [17] W. Hönig and N. Ayanian, *Flying Multiple UAVs Using ROS*. Springer International Publishing, 2017, pp. 83–118. [Online]. Available: https://doi.org/10.1007/978-3-319-54927-9_3